

# Theoretical Study on a Novel Series of Fullerene-Containing Organometallics $\text{Fe}(\eta^5\text{-C}_{55}\text{X}_5)_2$ ( $\text{X} = \text{CH}, \text{N}, \text{B}$ ) and Their Large Third-Order Nonlinear Optical Properties

Yan-Chun Liu,<sup>†</sup> Yu-He Kan,<sup>‡</sup> Shui-Xing Wu,<sup>†</sup> Guo-Chun Yang,<sup>†</sup> Liang Zhao,<sup>†</sup> Min Zhang,<sup>†</sup> Wei Guan,<sup>†</sup> and Zhong-Min Su<sup>\*†</sup>

*Institute of Functional Material Chemistry, Faculty of Chemistry, Northeast Normal University, ChangChun 130024, People's Republic of China, and Department of Chemistry, Huaiyin Teachers College, Jiangsu Province Key Laboratory for Chemistry of Low-Dimensional Materials, Huaian 223300, People's Republic of China*

*Received: February 2, 2008; Revised Manuscript Received: June 24, 2008*

Geometry structures, electronic spectra, and third-order nonlinear optical (NLO) properties of  $\text{Fe}(\eta^5\text{-C}_{55}\text{X}_5)_2$  ( $\text{X} = \text{CH}, \text{N}, \text{B}$ ) have first been investigated by time-dependent density functional theory. We analyzed the intramolecular interactions between ferrocene and the  $\text{C}_{50}$  moiety. The calculated electronic absorption spectrum indicates that the short wavelength transitions are ascribed to the  $\text{C}_{50}$  moiety mixed charge transfer transition of ferrocene itself, while the low energy excitation transitions are ascribed to the unique charge transfer transition from ferrocene to  $\text{C}_{50}$  moiety in these systems. The third-order polarizability  $\gamma$  values based on sum of states (SOS) method show that this class of ferrocene/fullerene hybrid molecule possesses a remarkably large third-order NLO response, especially for  $\text{Fe}(\eta^5\text{-C}_{55}\text{B}_5)_2$  with the static third-order polarizability ( $\gamma_{\text{av}}$ ) computed to be  $-10410 \times 10^{-36}$  esu and the intrinsic second hyperpolarizability to be 0.250. Thus, these complexes have the potential to be used for excellent third-order nonlinear optical materials. Analysis of the major contributions to the  $\gamma_{\text{av}}$  value suggest that the charge transfer from ferrocene to  $\text{C}_{50}$  moiety along the  $z$ -axis (through Fe atom and the centers of two hybrid fullerenes) play the key role in the NLO response. Furthermore, boron substitution is an effective way of enhancing the optical nonlinearity compared to CH and N substitution, owing to smaller energy gap and better conjugation through the whole molecule.

## Introduction

In 1987, Green et al. showed ferrocene derivatives providing highly efficient second harmonic generation (SHG);<sup>1</sup> since then, the large nonlinear optical properties of organometallic compounds have attracted the attention of an increasing number of scientists.<sup>2,3</sup> Organometallic compounds can provide polarizable electrons and have metal-to-ligand or ligand-to-metal charge-transfer bands in the UV–visible region. Furthermore, the modification of organic fragments can allow us to explore new materials for the engineering of nonlinear optical (NLO) hyperpolarizabilities.<sup>4</sup> Ferrocene is an 18-electron organometallic compound, which is composed of a pair of  $\eta^5\text{-6}\pi$ -electron aromatic pentagonal carbon ligands (cyclopentadienide = Cp) and  $d^6$ -electron iron(II) atom,<sup>5,6</sup> and as a useful design motif, it was always employed to deliver the targeted property.<sup>7</sup> On the one hand, due to the excellent electron-donating ability of ferrocene, materials suitable for SHG have been yielded;<sup>1,8</sup> on the other hand, the third-order NLO materials<sup>9</sup> and potential multiphoton absorption materials<sup>10</sup> have also been obtained on the basis of ferrocene.

Since the discovery of  $\text{C}_{60}$ ,<sup>11</sup> the unique properties of fullerenes have attracted wide investigational interest from both experimental and theoretical chemists.<sup>12</sup> Fullerene is a fascinating molecule because of a large number of conjugated double bonds, which lead us to expect large nonlinear polarizabilities.<sup>13</sup>

But the third-order polarizabilities of  $\text{C}_{60}$ <sup>14</sup> ( $7.5 \times 10^{-34}$  esu) and ferrocene<sup>15</sup> ( $9.7 \times 10^{-35}$  esu) are not as large as expected at the beginning. However, the large third-order optical polarizabilities can be obtained by ferrocene or  $\text{C}_{60}$  interacting with extensively conjugated  $\pi$ -electron systems.<sup>16,17</sup> Typically, ferrocene covalently linked  $\text{C}_{60}$ -based exist well intramolecular charge transfer.<sup>18</sup> Hauke and co-workers reported the synthesis and properties of a D–A dyad involving a directly bonded donor ferrocene connected to the electron-accepting azafullerene group, in which a large and evident intramolecular charge transfer (ICT) has been observed.<sup>19</sup> Generally, larger nonlinear optical response is exhibited by intramolecular charge transfer compounds.<sup>2,20</sup>

Some scientists made great efforts to prepare fullerene dimers and polymers, in which  $\text{C}_{60}$  units are linked by nonmetallic<sup>21</sup> or metallic<sup>22</sup> atoms, and expected to obtain some materials with particular properties.<sup>23</sup> However, connected by a transition metal bridge, these dimers are not perfect  $\eta^5$ - or  $\eta^6$ -coordination.<sup>24</sup> Recently, Nakamura et al. reported the first successful syntheses of ferrocene/fullerene hybrid molecules.<sup>25,26</sup> In these molecules, the five Cp carbons represent one pentagon of  $\text{C}_{60}$ , isolated from the remaining 50  $\text{sp}^2$  carbon atoms by five surrounding  $\text{sp}^3$  carbon atoms each bearing a phenyl group or others. Namely, connected by a  $\eta^5$ -coordinated metal atom, a cyclopentadienide cycle and fullerene unit can form “bucky metallocenes”, in which the homoconjugativity effect through  $\text{sp}^3$  carbon atoms allows electronic communication between ferrocene and “bowl-shaped”  $\text{C}_{50}$  moiety in these “bucky metallocenes”.<sup>27</sup> Enlightened by experiment, Stankevich et al. calculated the  $\text{Fe}(\eta^5\text{-CorH}_5)_2$  system as a simplified mode using HF/3–21 g method, and predicted the possibility of the existence of such compounds with a iron atom sandwiched between two fullerene units.<sup>28</sup>

\* To whom correspondence should be addressed. Fax: 86-431-85684009. E-mail: zmsu@nenu.edu.cn.

<sup>†</sup> Institute of Functional Material Chemistry, Faculty of Chemistry, Northeast Normal University.

<sup>‡</sup> Department of Chemistry, Huaiyin Teachers College, Jiangsu Province Key Laboratory for Chemistry of Low-Dimensional Materials.

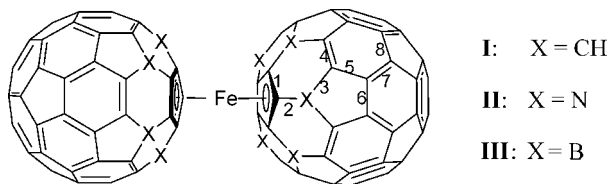


**Figure 1.** Calculation models within  $D_{5d}$  symmetry.

Here, irritated by experimental and theoretical work mentioned above, and for pursuing large conjugated system and then large third-order NLO properties, we discussed the two fullerenes ( $\text{C}_{60}\text{H}_5^-$ ) sandwiched iron(II) compound by using density functional theory method. Furthermore, considering atom N and B can facilitate better orbital interaction than the group CH, we designed two more systems in which the carbon atoms at  $\alpha$ -position of a five-membered cycle were replaced by five atoms N and B, respectively. The intramolecular orbital interaction and the electronic absorption spectra of these three systems have been theoretically investigated, and the third-order polarizabilities were calculated by the sum-overstates (SOS) formula. Meanwhile, the intrinsic second hyperpolarizabilities developed by Kuzyk<sup>29</sup> were calculated here.

### Theoretical Methods and Calculated Models

Density functional theory (DFT) calculations reported here were performed with the ADF 2006.01 program.<sup>30</sup> For geometrical optimization of all systems, we used the local density approximation (LDA) characterized by the functional of Vosko–Wilk–Nusair (VWN) parametrization for correlation functional and Beck<sup>31</sup> and Perdew<sup>32</sup> nonlocal corrections were used for the exchange and correlation energy, respectively. The electronic absorption spectra were calculated based on the time-dependent density functional theory (TDDFT), where the adiabatic local density approximation (ALDA) was used and the van Leeuwen–Baerends potential (LB94)<sup>33</sup> that corrects the LDA potential in the outer region of the molecule was also performed. TDDFT has been proved with its efficiency in the evaluation of electronic spectra for a wide range of compounds. In our calculations, we used triple- $\zeta$  plus polarization (TZP) STO basis set for electrons of all atoms. The zero order regular approximation (ZORA)<sup>34</sup> was adopted to account for the relativistic effects of the most inert (core) electrons. Herein, three molecules were shown in Figure 1.

The third-order polarizabilities were then calculated by using the sum-overstates (SOS) formula.<sup>35</sup> The expression of third-order polarizabilities  $\gamma$  can be obtained by application of time-dependent perturbation theory to the interacting electromagnetic field and microscopic system, as described in the following.

$$\gamma_{ijkl} = \frac{4\pi^2}{3\hbar^3} P(i,j,k,l; -\omega_\sigma, \omega_1, \omega_2, \omega_3) \times$$

$$\sum_{m \neq g} \sum_{n \neq g} \sum_{p \neq g} \left[ \frac{(\mu_i)_{gm} (\bar{\mu}_j)_{mn} (\bar{\mu}_k)_{np} (\mu_l)_{pg}}{(\omega_{mg} - \omega_\sigma - i\Gamma_{mg})(\omega_{ng} - \omega_1 - \omega_2 - i\Gamma_{ng})} \right. \\ \left. \frac{(\mu_l)_{pg} (\mu_k)_{ng} (\mu_j)_{mg} (\mu_i)_{gm}}{(\omega_{pg} - \omega_3 - i\Gamma_{pg})} \right]$$

$$\sum_{m \neq g} \sum_{n \neq g} \left[ \frac{(\mu_i)_{gm} (\mu_j)_{mg} (\mu_k)_{gn} (\mu_l)_{ng}}{(\omega_{mg} - \omega_\sigma - i\Gamma_{mg})(\omega_{ng} - \omega_2 - i\Gamma_{ng})(\omega_{ng} - \omega_3 - i\Gamma_{pg})} \right]$$

Here,  $\omega_\sigma = \omega_1 + \omega_2 + \omega_3$  is the polarization response frequency,  $i,j,k,l$  is the Cartesian coordinates.  $P(i,j,k,l;$

$\omega_\sigma, \omega_1, \omega_2, \omega_3)$  indicates all permutations of  $(\omega_\sigma, i)$ ,  $(\omega_1, j)$ ,  $(\omega_2, k)$ ,  $(\omega_3, l)$ , all together 24.  $(\mu_i)_{gm}$  is an electronic transition moment along the  $i$  axis of the Cartesian system, between the ground state  $|g\rangle$  and the excited state  $|m\rangle$ ;  $(\bar{\mu}_j)_{ng}$  is the dipole difference equal to  $(\mu_j)_{mn} - (\mu_j)_{gg}$ ;  $\hbar\omega_{ng}$  is the transition energy from  $|g\rangle$  state to  $|n\rangle$  state;  $\Gamma_{mg}$  is damping factor whose value lies on the width of energy levels, and, in the calculation of nonresonant third-order nonlinear optical properties, the  $\Gamma_{mg} = \Gamma_{ng} = \Gamma_{pg} = 0$  is supposed. As input parameters for the SOS formula to calculate the third-order polarizabilities, the transition energies, transition moments and dipole moments were obtained from the calculated results based on the EXCITATION model of ADF program. 300 excited states were calculated for the third-order polarizabilities, and the amount was enough according to the converge curves of SOS method (Figure S1 in Supporting Information).

### Results and Discussions

**Molecular Structures.** Xu et al. studied the first-row transition-metal metallocenes using a broad range of density functional methods and discovered that BP86 method give ferrocene structures in good agreement with experiment.<sup>36</sup> Before discussing the title compounds, we optimized the geometry of ferrocene ( $D_{5h}$ -Fe(Cp)<sub>2</sub>) by using BP86 functional employing TZP basis set for all electron of atoms. The calculated Fe–C (2.054 Å) and C–C (1.436 Å) bond distances are closer to the experiment<sup>37</sup> values than reported.<sup>36</sup> After optimization of the title compounds  $\text{Fe}(\eta^5\text{-C}_{55}\text{X}_5)_2$  (X = CH, N, B), both  $D_{5h}$  and  $D_{5d}$  conformations are locally stable ( $N_{\text{img}} = 0$ ) for compounds **I** and **II**, but except compound **III** with one imaginary frequency of 15i  $\text{cm}^{-1}$  and two smaller ones of 5i  $\text{cm}^{-1}$  at  $D_{5h}$  and  $D_{5d}$  conformations, respectively. Additionally, compounds **I** and **II** possess energy differences of 1.66 and 2.34 kcal/mol between  $D_{5h}$  and  $D_{5d}$  conformations respectively, which are larger than the one in ferrocene obtained by theory<sup>38</sup> and experiment.<sup>37</sup> Now, in order to facilitate discussion on orbital interactions and compare with other reported analysis on the ferrocene molecule, the sections below will mainly describe  $D_{5d}$  conformations for all compounds.

The main calculated geometry parameters of the three systems are listed in Table 1 and compared with experimental values. Other unlisted bond distances of three molecules are close to each other and to experimental values (most differences within 0.004 Å). From bond 5 to bond 8, the distances in the systems **I** and **II** are close to experimental values of  $\text{FeC}_{60}\text{Ph}_5\text{Cp}$  molecule. For system **I**, bond 2 and bond 3 are shorter than experimental values. This may be explained in terms of the special repulsions among the five phenyl groups in  $\text{FeC}_{60}\text{Ph}_5\text{Cp}$ , which elongate the corresponding bond distances. Without impact of five phenyl groups on homoconjugation effect in system **I**, the distance of bond 4 is elongated, and bonds 2, 3 and 4 are inclined to be averaged. For system **II**, the C–N bond distance is shorter than the corresponding C–C bond distance, and distances through bond 1 to bond 8 are more equalized, while in the boron atom substituted system, these bond lengths are more uneven than those in system **I**. Consequently, in  $\text{Fe}(\eta^5\text{-C}_{55}\text{N}_5)_2$ , the five-member rings isolated by nitrogen atoms have good conjugation effect with the other carbon atoms of the fullerene moiety, thus the Fe–C bond distance increased. However, contrary to system **II**, the isolated pentagon of the boron substituted fullerene is more isolated and the Fe–C bond distances are shortened in system **III**.

Additionally, the H atoms of the cyclopentadienyl rings are all equivalent, the C–H bonds in ferrocene are bent a certain

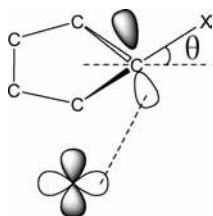
**TABLE 1: Selected Bond Distances (Å) of Optimized Structures, and Corresponding Determination by Experiment**

molecule	Fe–C	distances between C–C or C–X at [60]fullerene							
		(1)	(2)	(3)	(4)	(5)	(6)	(7)	(8)
<b>I</b> ( $D_{5d}$ )	2.082	1.432	1.508	1.542	1.385	1.438	1.453	1.403	1.440
<b>II</b> ( $D_{5d}$ )	2.114	1.426	1.418	1.437	1.395	1.428	1.443	1.411	1.434
<b>III</b> ( $D_{5d}$ )	2.064	1.456	1.545	1.571	1.403	1.451	1.475	1.410	1.453
FeC <sub>60</sub> Ph <sub>5</sub> Cp <sup>39</sup>	2.083	1.432	1.517	1.547	1.371	1.442	1.451	1.394	1.441

**TABLE 2: Energy Decomposition Analysis for Systems I, II, III, and Ferrocene at BP86/TZP (energy unit: kcal/mol)**

term	Fe(Cp) <sub>2</sub> ( $D_{5d}$ )	<b>I</b> ( $D_{5d}$ )	<b>II</b> ( $D_{5d}$ )	<b>III</b> ( $D_{5d}$ )
$\Delta E_{\text{int}}$	−893.2	−765.6	−712.9	−708.1
$\Delta E_{\text{Pauli}}$	270.0	254.8	226.2	260.4
$\Delta E_{\text{elstat}}$	−591.6 (50.9%) <sup>a</sup>	−358.2 (35.1%)	−288.0 (30.7%)	−331.6 (34.2%)
$\Delta E_{\text{orb}}$	−571.7 (49.1%) <sup>a</sup>	−662.3 (64.9%)	−651.1 (69.3%)	−636.9 (65.8%)

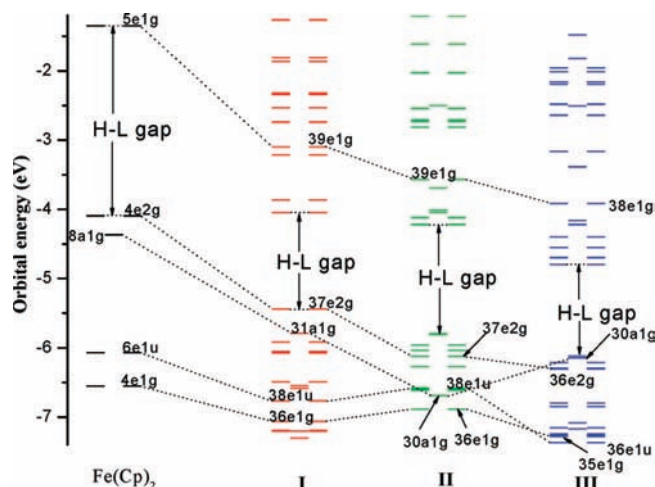
<sup>a</sup> Percentage of attractive interactions ( $\Delta E_{\text{elstat}} + \Delta E_{\text{orb}}$ ).

**Figure 2.** Sketch for the angle ( $\theta$ ) of X displaced away from the Cp<sup>−</sup> ring.

angle  $\theta$  out of the plane of the C<sub>5</sub> ring toward the metal iron atom. The angle  $\theta$  determined by gas-phase electron diffraction in experiment is 3.7°;<sup>40</sup> which is only 1.7°,<sup>41</sup> determined by Neutron diffraction. The calculated value is 0.97° by using BP86/DZP.<sup>36</sup> In this work, the obtained value from the BP86/TZP is 0.9° for this angle of ferrocene at staggered model. This distortion angle is helpful to understand the orbital interaction between p<sub>z</sub> orbitals of Cp<sup>−</sup> and d orbitals of iron atom. As shown in Figure 2, the C–X bonds are bent out of plane far away from iron atom for a relatively larger angle (18.8°, 23.1°, 31.5° for X = CH, N, B, respectively), which certainly influence the orbital interactions of our systems (vide infra).

**Molecular Orbitals and Energy Levels.** Recently, Kang et al. studied C<sub>60</sub>-ferrocene hybrid system C<sub>60</sub>(CH<sub>3</sub>)<sub>5</sub>FeCp and found a much more narrow HOMO–LUMO gap than ferrocene, which was caused by the  $\pi^*$  orbitals of C<sub>60</sub>(CH<sub>3</sub>)<sub>5</sub> inserted under the LUMO of ferrocene.<sup>42</sup> The HOMO–LUMO gaps of systems **I–III** are 1.39 eV, 1.58 and 1.33 eV, respectively. All these values are much smaller than the gap of ferrocene (2.75 eV). When compared with ferrocene (shown in Figure 3), we found the decreased corresponding energy levels, between which some dominant orbitals of conjugated C<sub>50</sub> moiety lied, and some other orbitals (such as LUMO of system **II**) with strong interactions between the ferrocene and the conjugated C<sub>50</sub> moiety came forth.

The diagrams for frontier molecular orbitals (FMOs) of our systems are given in Figure 4, and some differences between FMOs of systems **I, II, and III** are clearly seen. The HOMO of system **I** is 37e2g, dominantly comes from d<sub>z<sup>2</sup>−y<sup>2</sup></sub> orbital of iron atom; the HOMO of system **II** is 29a2u, whose contribution is mainly from the nonbonding orbits of nitrogen atoms and delocalization over the fullerenes; and for system **III**, the middle 40 carbon atoms of fullerene largely contributed to the HOMO, which is 10a2g. The LUMOs of both system **I** and its isoelectronic system **II** are 38e1g, mainly come from the contribution of C<sub>50</sub> moiety, but the orbitals on ferrocene moiety partly contributed to the LUMO of system **II**. The cross energy

**Figure 3.** Correlation between energy levels of corresponding orbital for systems **I, II, III**, and Fe(Cp)<sub>2</sub> (within  $D_{5d}$  symmetry). “H–L gap” denotes that HOMOs lie underside and LUMOs lie upside.

levels exist in system **III**, and the LUMO of system **III** is 36e2u, which is different from the systems **I** and **II**, and come from the conjugated p– $\pi^*$  interaction between the boron atoms and the carbon atoms resided at C<sub>50</sub> moiety. These differences between corresponding FMOs indicate that different electronic properties will come forth upon a given external electronic field.

**Energy Decomposition Analysis (EDA).** The interactions between the metal atoms and fullerene fragments have been analyzed by means of the energy decomposition analysis implemented in ADF package, which is based on the EDA method.<sup>43</sup> The instantaneous interaction energy ( $\Delta E_{\text{int}}$ ) between the two fragments can be divided into three main components:

$$\Delta E_{\text{int}} = \Delta E_{\text{Pauli}} + \Delta E_{\text{elstat}} + \Delta E_{\text{orb}}$$

Here,  $\Delta E_{\text{Pauli}}$  is the repulsive four-electron interactions between occupied orbitals,  $\Delta E_{\text{elstat}}$  gives the electrostatic interaction energy between the unperturbed charge distributions of the prepared fragments, and  $\Delta E_{\text{orb}}$  corresponds to the stabilizing orbital interaction term.

Table 2 gives the results of energy decomposition analysis for systems **I–III** and ferrocene within  $D_{5d}$  symmetry. Ferrocene is a closed shell system and the electronic configuration of Fe<sup>2+</sup> ion was accepted as (a<sub>1g</sub>)<sup>2</sup>(e<sub>2g</sub>)<sup>4</sup>(e<sub>1g</sub>)<sup>0</sup>. It is well-known that the most important orbital interactions in ferrocene arise from the (e<sub>1g</sub>) Cp<sup>−</sup> → Fe<sup>2+</sup>  $\pi$ -type back-donation. The orbital interactions of our three systems also mainly come from the e<sub>1g</sub>  $\pi$ -donation. The data collected in table 2 show that the orbital interaction

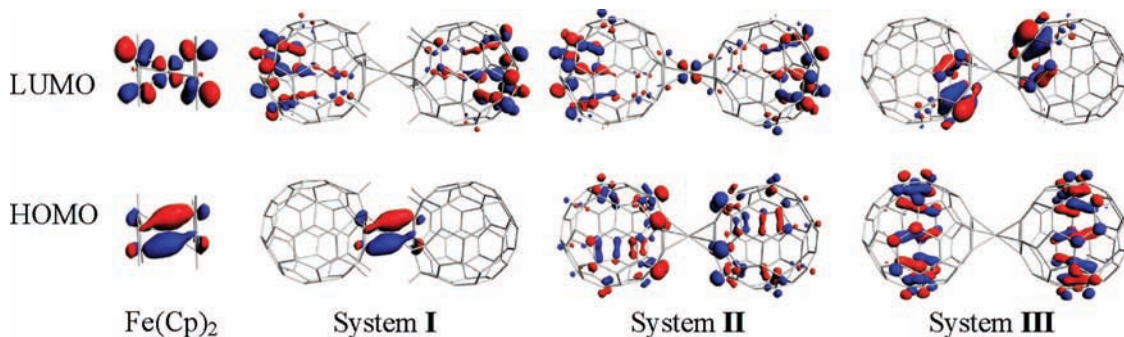


Figure 4. HOMO and LUMO diagrams for systems I, II, and III, in comparison with  $\text{Fe}(\text{Cp})_2$  (within  $D_{5d}$  symmetry).

TABLE 3: Charge Attached on the Selected Atoms, Calculated by NBO 3.1

atom	$\text{Fe}(\text{Cp})_2$ ( $D_{5d}$ )	I ( $D_{5d}$ )	II ( $D_{5d}$ )	III ( $D_{5d}$ )
X	0.263 <sup>a</sup>	-0.277	-0.395	0.828
Ccp <sup>b</sup>	-0.282	-0.038	0.12	-0.336
Fe	0.185	0.224	0.188	0.331

<sup>a</sup> Charge attached on atom H, <sup>b</sup> Atom C resided in  $\text{Cp}^-$  ring.

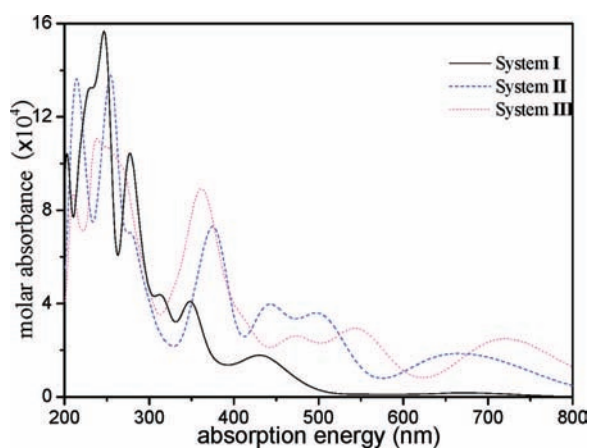


Figure 5. Electronic absorption spectrum calculated by TDDFT at the level of LB94/TZP.

energies between  $\text{Fe}^{2+}$  and fullerene fragment in the systems I, II, and III are larger than one in ferrocene by 60~100 kcal/mol, which is caused by the lower corresponding orbital energy levels of the fullerene fragment than a single Cp cycle, and then better orbital correlation with  $\text{Fe}^{2+}$  ion. The orbital interaction energies of systems I, II, and III are in the order of  $\text{I} > \text{II} > \text{III}$ , which seems to be consistent with conclusion of analysis on the angle  $\theta$  mentioned above (vide supra): the trend of the distorted angle is  $\text{B} > \text{N} > \text{CH}$ .

However, because of the dispersed distribution of charge in the fullerene fragment, the  $\Delta E_{\text{elstat}}$  value in our three systems compared with ferrocene decreases by more than 230 kcal/mol. In order to illustrate the electrostatic interaction in more detail, natural population analysis (NPA) was carried out by NBO 3.1,<sup>44</sup> and selected values are detailed in Table 3. We can find that the smallest electrostatic interaction in system II is due to positive carbon atoms of Cp ring endowed by large electronegativity of the nitrogen atom, and for system III, although there are considerable amount of opposite charges between the carbon atoms of Cp ring and iron atom, the electrostatic interaction is no larger than that in system I, which is possibly ascribed to the electrostatic repulsion between the iron atom and comparatively positive boron atoms neighboring to the Cp ring.

**Electronic Absorption Spectrum.** On the basis of the optimized geometry structures, we used TDDFT to calculate

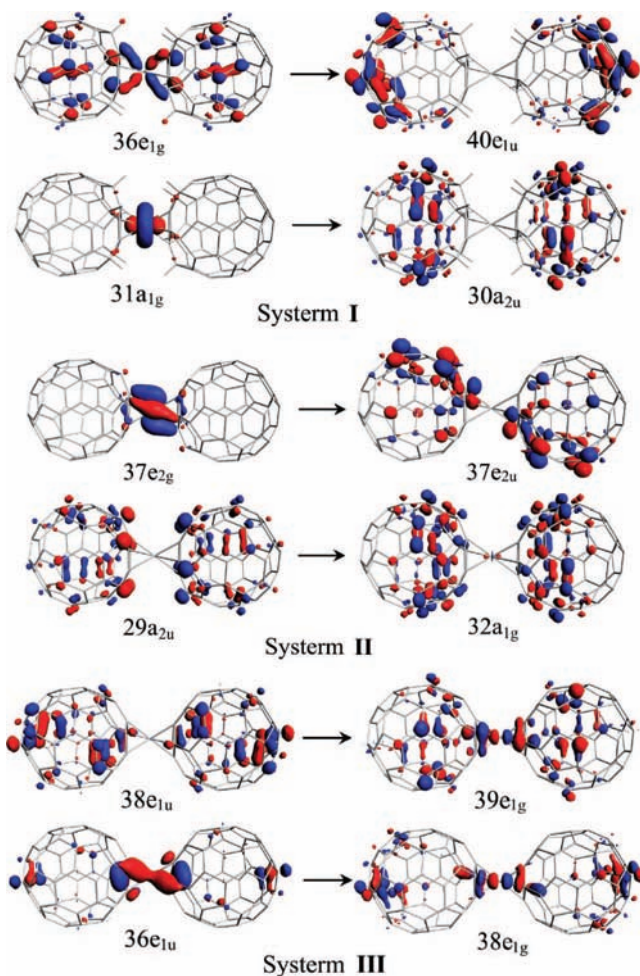
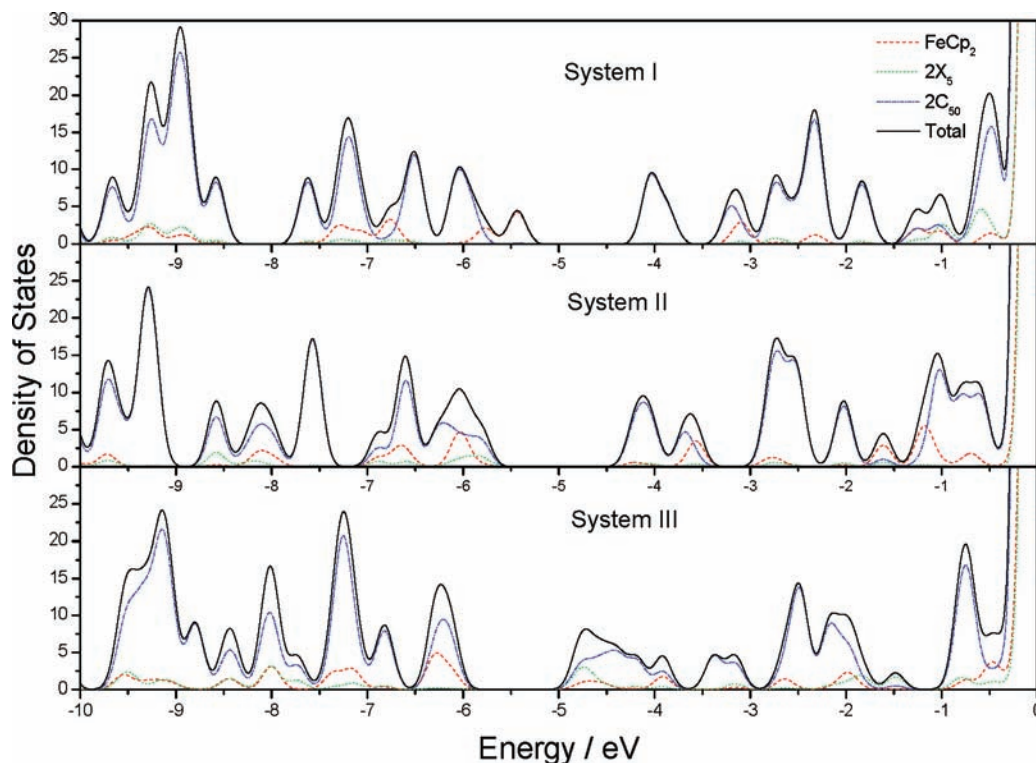


Figure 6. Molecular orbital diagram related with correlative excitation transition states of systems I, II, and III.

the electronic spectrum. The local density approximation (LDA) was used, and the LDA potential was corrected by the Van Leeuwen–Baerends potential (LB94). The electronic absorption spectrums (fitted with Gaussian function) of the three molecules are shown in Figure 5. Taking system I as an example, there are strong absorptions under 400 nm, where the four major bands at 251, 280, 341, and 380 nm correspond to the 258, 273, 350, and 390 nm of  $\text{C}_{60}\text{Ph}_5\text{H}^{25}$  which are contributed from the fullerene moiety itself, and another absorption peak at 317 nm contributed from the conjugated “bowl-shaped”  $\text{C}_{50}$  moiety, which has not been pointed out in experiment of  $\text{C}_{60}\text{Ph}_5\text{H}$ . Additionally, there are three absorption bands coming from the charge transfer (CT) absorption located in ferrocene fragment at red-shifted 201, 277, and 350 nm from 200, 265, and 324 nm of an individual ferrocene molecule, respectively,<sup>5</sup> which



**Figure 7.** Density-of-States plots for systems **I**, **II**, **III**; each molecule was divided into three fragments: FeCp<sub>2</sub>, 2X<sub>5</sub>, and 2C<sub>50</sub>.

is resulted from the corresponding orbitals not only locating over ferrocene in system **I**.

Noticeably, both 10A<sub>2u</sub> and 11A<sub>2u</sub> absorption states at 438 and 418 nm are ascribed to the 36e<sub>1g</sub> → 40e<sub>1u</sub> transition, and the 1A<sub>2u</sub> state at 676 nm has weak absorbance, which is ascribed to the 31a<sub>1g</sub> → 30a<sub>2u</sub> transition. Seen from Figure 6, it is the charge transfer between ferrocene fragment and conjugated C<sub>50</sub> moiety that was displayed as remarkable and peculiar features of these transitions for our studied systems. Systems **II** and **I** are isoelectronic, however, the red shift for system **II** is resulted from the nitrogen atoms bearing lone pairs which facilitate communication between ferrocene fragment and conjugated C<sub>50</sub> moiety better than CH groups. In system **II**, 1A<sub>2u</sub> state contributed from 31a<sub>1g</sub> → 30a<sub>2u</sub> transition red shift to 719 nm, and the peculiar charge transfer transition (the absorption peak at 378 nm contributed from 37e<sub>2g</sub> → 37e<sub>2u</sub> transition) of system **II** is enhanced, and the absorption at 645 nm includes *n* →  $\pi^*$  transition (3A<sub>2u</sub>: 29a<sub>2u</sub> → 32a<sub>1g</sub>), which does not appear in system **I**. For system **III**, excellent orbital interactions between ferrocene fragment and the conjugated C<sub>50</sub> moiety at the two ends are shown in Figure 6, where the feature of 6e<sub>1u</sub> in ferrocene molecule exists in both 38e<sub>1u</sub> and 36e<sub>1u</sub>, and the feature of 5e<sub>1g</sub> in both 39e<sub>1g</sub> and 38e<sub>1g</sub>. The strong interactions between the molecular orbitals play an important role in the electron exciting process. The absorption state at 370 nm is mainly contributed from the 38e<sub>1u</sub> → 39e<sub>1g</sub> transition, and absorption at 547 nm mainly is contributed from the 36e<sub>1u</sub> → 38e<sub>1g</sub>. It is clear that systems **I** and **II** have similar transition natures, which are the charge-transfer transitions from ferrocene to other moieties, but system **III** does not.

**Third-Order Nonlinear Optical Properties.** According to discussion on the electronic transitions, we can assign the systems **I**, **II**, and **III** as models of A–B–D–B–A, A–D'–D–D'–A, and A–A'–D–A'–A (D: donor, A: acceptor, and B: block), respectively. Therefore, such compounds are expected to possess good NLO response, and activate us to investigate

**TABLE 4: Calculated Results of the Third-Order Polarizabilities (Unit: 10<sup>-36</sup> esu) of the Systems with TD-SOS**

	system <b>I</b>	system <b>II</b>	system <b>III</b>
$\gamma_{xxxx}$	-783.5	-1304	-842.9
$\gamma_{xxzz}$	-993.4	-2210	-2116
$\gamma_{zzzz}$	-11,330	-33,390	-46,960
$\gamma_{av}$	-2,820	-7,823	-10,410

their second hyperpolarizabilities due to their molecule symmetries. Here, we calculated the static second hyperpolarizabilities  $\gamma$  by using TDDFT followed SOS (TD-SOS) method. We took ferrocene as a reference compound, and calculated its 30 allowed excited states. Then using the sum-overstates (SOS) formula, we got its third-order polarizabilities of *D*<sub>5h</sub>(*D*<sub>5d</sub>)-Fe(Cp)<sub>2</sub> 24.5(25.1) × 10<sup>-36</sup> esu, which is comparable with its experimental values 96.7 × 10<sup>-36</sup> esu and theoretical values 24.6 × 10<sup>-36</sup> esu calculated by CNDO method.<sup>15,16,45</sup> It is apparent that our method employed to calculate the second hyperpolarizabilities  $\gamma$  in this paper is effective and reliable. For the title compounds, the 300 allowed excited states were calculated and those physical values were then taken into SOS formula to calculate the third-order polarizabilities well converged. The  $\gamma$  values of three systems are listed in Table 4. All of the systems have considerable third-order polarizabilities, especially for system **III**. Our investigation indicates that, for our systems, the NLO response can be remarkably enhanced by the boron atom, thanks to its role as acceptor unit, as well as its facility for extended  $\pi$ -system. It is hoped that the results presented in this paper will give some hint to experimental research in the field of NLO properties.

On the basis of NPA description (*vide supra*), we can find C<sub>50</sub> carry charge of 0.03, 1.28, and -2.68 in systems **I**, **II**, and **III**, respectively. As a result, system **III** get more charge for delocalization and polarization, which may make system **III** better NLO response. Moreover, in order to analyze the orbital population of each molecular fragment, we introduced density

of states (DOS). As can be seen from the overlap-population DOS plot (Figure 7), the frontier MOs of system I were mainly from the ferrocene and the two C<sub>50</sub> moieties, and other energy regions also present the dominant contribution of certain molecular fragments; However, the LUMOs of system II are mainly distributed to the two C<sub>50</sub> moieties, and the MO distribution of system III is not clearly. As seen from Figure 7, the CH clusters of system I give good partition between ferrocene and C<sub>50</sub> moieties; the nitrogen atoms in system II is secondary; the boron atoms in system III are somewhat different from CH cluster and nitrogen owing to the strong orbitals interactions between the ferrocene and C<sub>50</sub> moieties. These results show that the delocalization of system III is better than systems I and II, which also makes system III have larger static third-order polarizability ( $\gamma$ ) values than both of I and II.

Furthermore, in order to understand the fundamental property of a molecule and remove size effects and allow molecules of drastically differing sizes to be compared directly, the intrinsic second hyperpolarizabilities developed by Kuzyk<sup>29</sup> were calculated here. This intrinsic property is determined by the ratio between the calculated value and the fundamental limit.<sup>46</sup> The fundamental limit of  $\gamma$  is bounded by

$$-\frac{e^4 \hbar^4}{m^2} \left( \frac{N^2}{E_{10}^5} \right) \leq \gamma \leq 4 \frac{e^2 \hbar^4}{m^2} \left( \frac{N^2}{E_{10}^5} \right)$$

where  $N$  is the number of electrons in the system,  $m$  is the electron mass,  $e$  is the electron charge, and  $\hbar$  is Planck's constant. The negative limit is for a centrosymmetric molecule, and the positive limit for an asymmetric molecule.

In this work, the systems I, II, and III give 50 sp<sup>2</sup> carbon atoms on each "bowl-shaped" C<sub>50</sub> moiety and 6 delocalized electrons on each Cp<sup>-</sup> ring, and 6 d electrons on iron(II) ion ( $N = 118$ ). We obtained their limits of second hyperpolarizabilities 35348, 39114, 41633  $\times 10^{-36}$ esu, respectively. The evaluated intrinsic third-order polarizability of the title compounds achieve values about 0.079, 0.200, and 0.250 for I, II, and III, respectively (Table S1 in Supporting Information), which accorded with the trends of computed absolute second hyperpolarizability  $\gamma$ . The results presented herein indicate molecular designing can drive nonlinear second hyperpolarizability approaching the physical limit.

## Conclusions

The present DFT calculations provide the following conclusions: (1) When compared with experiment results, systems I and II are stable and can be synthesized in certain experimental conditions, and system III with little barrier for rotating axially is stable within lower symmetry. (2) The mutual crossing orbital energy levels of ferrocene and C<sub>50</sub> moieties result in the HOMO–LUMO gap decreasing, and energy levels are serried; An analysis of orbitals interactions between iron (II) ion and C<sub>55</sub>X<sub>5</sub><sup>-</sup> ligand using EDA shows that the orbital interaction energies of systems I, II, and III are in the order of I > II > III, the trend of electrostatic interaction is I > III > II. (3) On the basis of the optimized geometry structures, we used LB94/TDDFT to calculate the electronic spectrum. The results indicate that the short wavelength transitions are ascribed to the C<sub>50</sub> moiety mixed charge transfer transitions of ferrocene itself, while the long wavelength transitions are ascribed to the unique charge transfer transition from ferrocene to C<sub>50</sub> moiety of these systems. (4) On the basis of the peculiar character of charge transfer of systems I, II, and III, we probed the NLO properties and origins of them. The  $\pi$ -conjugation of systems II and III

is stronger than system I, which results in increasing charge transfer character, and then larger the value of  $\gamma$ , in systems II and III; furthermore, the DOS of system III is evenly delocalized among molecule fragments, the delocalization of charge is better than systems I and II. Therefore, its  $\gamma$  value is the largest in system III. Additionally, the evaluated intrinsic third-order polarizability of the title compounds achieve values about 0.079, 0.200, and 0.250 for I, II, and III respectively, which meet the trends of computed absolute second hyperpolarizability  $\gamma$ .

**Acknowledgment.** The authors acknowledge the financial support from the National Natural Science Foundation of China (Project Nos. 20573016), Training fund of NENU's Scientific Innovation Project (NENU-STC07017) and Science Foundation for Young Teachers of Northeast Normal University (20070304), and are supported by Program for Changjiang Scholars and Innovative Research Team in University (PCSIRT).

**Supporting Information Available:** Convergent behaviors of SOS calculations for the static third-order polarizabilities and detailed data drawn for calculating intrinsic hyperpolarizability. This information is available free of charge via the Internet at <http://pubs.acs.org>.

## References and Notes

- (1) Green, M. L. H.; Marder, S. R.; Thompson, M. E.; Bandy, J. A.; Bloor, D.; Kolinsky, P. V.; Jones, R. J. *Nature* **1987**, *330*, 360.
- (2) Nalwa, H. S. *Appl. Organomet. Chem.* **1991**, *5*, 349.
- (3) (a) Long, N. J. *Angew. Chem., Int. Ed. Engl.* **1995**, *34*, 21. (b) Whittall, I. R.; McDonagh, A. M.; Humphrey, M. G.; Samoc, M. Organometallic complexes in nonlinear optics II: Third-order nonlinearities and optical limiting studies. In *Advances in Organometallic Chemistry*; West, R., Hill, A. F. Eds.; Academic Press: New York, 1999; Vol. 43, pp 349. (c) Cariati, E.; Pizzotti, M.; Roberto, D.; Tessore, F.; Ugo, R. *Coord. Chem. Rev.* **2006**, *250*, 1210.
- (4) Calabrese, J. C.; Cheng, L. T.; Green, J. C.; Marder, S. R.; Tam, W. J. *Am. Chem. Soc.* **1991**, *113*, 7227.
- (5) Gray, H. B.; Sohn, Y. S.; Hendrickson, N. J. *Am. Chem. Soc.* **1971**, *93*, 3603.
- (6) (a) Haaland, A. *Acc. Chem. Res.* **1979**, *12*, 415. (b) Ruhl, E.; Hitchcock, A. P. *J. Am. Chem. Soc.* **1989**, *111*, 5069.
- (7) (a) Fery-Forgues, S.; Delavaux-Nicot, B. *J. Photochem. Photobiol. A* **2000**, *132*, 137. (b) Debroy, P.; Roy, S. *Coord. Chem. Rev.* **2007**, *251*, 203. (c) Ashton, P. R.; Balzani, V.; Clemente-Leon, M.; Colonna, B.; Credi, A.; Jayaraman, N.; Raymo, F. M.; Stoddart, J. F.; Venturi, M. *Chem. Eur. J.* **2002**, *8*, 673. (d) Brettar, J.; Burgi, T.; Donnio, B.; Guillon, D.; Klappert, R.; Scharf, T.; Deschenaux, R. *Adv. Funct. Mater.* **2006**, *16*, 260. (e) Wolf, M. O. *Adv. Mater.* **2001**, *13*, 545. (f) Kumar, R.; Misra, R.; Prabhuraja, V.; Chandrashekar, T. K. *Chem. Eur. J.* **2005**, *11*, 5695. (g) Abd-Elzاهر, M. M.; El-Shiekh, S. M.; Eweis, M. *Appl. Organomet. Chem.* **2006**, *20*, 597. (h) Hudson, R. D. A. *J. Organomet. Chem.* **2001**, *637*, 47. (i) Abd-El-Aziz, A. S.; Todd, E. K. *Coord. Chem. Rev.* **2003**, *246*, 3.
- (8) (a) Wright, M. E.; Toplikar, E. G. *Macromolecules* **1992**, *25*, 6050. (b) Janowska, I.; Zakrzewski, J.; Nakatani, K.; Palusiak, M.; Walak, M.; Scholl, H. J. *Organomet. Chem.* **2006**, *691*, 323. (c) Togni, A.; Rihg, G. *Organometallics* **1993**, *12*, 3368. (d) Malaun, M.; Kowallick, R.; McDonagh, A. M.; Marcaccio, M.; Paul, R. L.; Asselberghs, I.; Clays, K.; Persoons, A.; Bildstein, B.; Fiorini, C.; Nunzi, J. M.; Ward, M. D.; McCleverty, J. A. *J. Chem. Soc., Dalton Trans.* **2001**, 3025. (e) Krishnan, A.; Pal, S. K.; Nandakumar, P.; Samuelson, A. G.; Das, P. K. *Chem. Phys.* **2001**, *265*, 313. (f) Barlow, S.; Bunting, H. E.; Ringham, C.; Green, J. C.; Bublitz, G. U.; Boxer, S. G.; Perry, J. W.; Marder, S. R. *J. Am. Chem. Soc.* **1999**, *121*, 3715. (g) Liao, Y.; Eichinger, B. E.; Firestone, K. A.; Haller, M.; Luo, J. D.; Kaminsky, W.; Benedict, J. B.; Reid, P. J.; Jen, A. K. Y.; Dalton, L. R.; Robinson, B. H. *J. Am. Chem. Soc.* **2005**, *127*, 2758. (h) Jayaprakash, K. N.; Ray, P. C.; Matsuoka, I.; Bhadbhade, M. M.; Puranik, V. G.; Das, P. K.; Nishihara, H.; Sarkar, A. *Organometallics* **1999**, *18*, 3851.
- (9) (a) Nalwa, H. S. *Mater. Lett.* **1997**, *33*, 23. (b) Hou, H. W.; Li, G.; Song, Y. L.; Fan, Y. T.; Zhu, Y.; Zhu, L. *Eur. J. Inorg. Chem.* **2003**, 2325. (c) Li, G.; Song, Y. L.; Hou, H. W.; Li, L. K.; Fan, Y. T.; Zhu, Y.; Meng, X. R.; Mi, L. W. *Inorg. Chem.* **2003**, *42*, 913. (d) Gonzalez-Cabello, A.; Claessens, C. G.; Martin-Fuch, G.; Ledoux-Rack, I.; Vazquez, P.; Zyss, J.; Agullo-Lopez, F.; Torres, T. *Synth. Met.* **2003**, *137*, 1487. (e) Mata, J. A.;

Peris, zjrn > E.; Llusar, R.; Uriel, S.; Cifuentes, M. P.; Humphrey, M. G.; Samoc, M.; Luther-Davies, B. *Eur. J. Inorg. Chem.* **2001**, 2113.

(10) (a) Zhang, X. B.; Feng, J. K.; Ren, A. M.; Sun, C. C. *J. Phys. Chem. A* **2006**, *110*, 12222. (b) Zheng, Q. D.; He, G. S.; Lu, C. G.; Prasad, P. N. *J. Mater. Chem.* **2005**, *15*, 3488. (c) Misra, R.; Kumar, R.; Chandrashekar, T. K.; Suresh, C. H.; Nag, A.; Goswami, D. *J. Am. Chem. Soc.* **2006**, *128*, 16083.

(11) Kroto, H. W.; Heath, J. R.; O'Brien, S. C.; Curl, R. F.; Smalley, R. E. *Nature* **1985**, *318*, 162.

(12) (a) Guldi, D. M.; Prato, M. *Acc. Chem. Res.* **2000**, *33*, 695. (b) Chen, Z. F.; King, R. B. *Chem. Rev.* **2005**, *105*, 3613. (c) Prato, M. *Top. Curr. Chem.* **1999**, *199*, 173. (d) Jensen, A. W.; Wilson, S. R.; Schuster, D. I. *Bioorg. Med. Chem.* **1996**, *4*, 767.

(13) (a) Chen, Q. Y.; Kuang, L.; Wang, Z. Y.; Sargent, E. H. *Nano Letters* **2004**, *4*, 1673. (b) Hamasaki, R.; Ito, M.; Lamrani, M.; Mitsuishi, M.; Miyashita, T.; Yamamoto, Y. *J. Mater. Chem.* **2003**, *13*, 21. (c) Tsuboya, N.; Hamasaki, R.; Ito, M.; Mitsuishi, M.; Miyashita, T.; Yamamoto, Y. *J. Mater. Chem.* **2003**, *13*, 511. (d) Wang, S. F.; Huang, W. T.; Liang, R. S.; Gong, Q. H.; Li, H. B.; Chen, H. Y.; Qiang, D. *Phys. Rev. B* **2001**, *63*, 15.

(14) Wang, Y.; Cheng, L. T. *J. Phys. Chem.* **1992**, *96*, 1530.

(15) Waite, J.; Papadopoulos, M. G. *J. Phys. Chem.* **1991**, *95*, 5426.

(16) Ghosal, S.; Samoc, M.; Prasad, P. N.; Tufariello, J. J. *J. Phys. Chem.* **1990**, *94*, 2847.

(17) Zhao, Y. M.; Shirai, Y.; Slepov, A. D.; Cheng, L.; Alemany, L. B.; Sasaki, T.; Hegmann, F. A.; Tour, J. M. *Chem. Eur. J.* **2005**, *11*, 3643.

(18) (a) Imahori, H.; Tamaki, K.; Yamada, H.; Yamada, K.; Sakata, Y.; Nishimura, Y.; Yamazaki, I.; Fujitsuka, M.; Ito, O. *Carbon* **2000**, *38*, 1599. (b) Guldi, D. M.; Maggini, M.; Scorrano, G.; Prato, M. *J. Am. Chem. Soc.* **1997**, *119*, 974. (c) Prato, M.; Maggini, M. *Acc. Chem. Res.* **1998**, *31*, 519. (d) Caporossi, F.; Floris, B.; Galloni, P.; Gatto, E.; Venanzi, M. *Eur. J. Org. Chem.* **2006**, 4362. (e) Oswald, F.; Islam, D. M. S.; Araki, Y.; Troiani, V.; de la Cruz, P.; Moreno, A.; Ito, O.; Langa, F. *Chem. Eur. J.* **2007**, *13*, 3924.

(19) Hauke, F.; Hirsch, A.; Liu, S. G.; Echegoyen, L.; Swartz, A.; Luo, C. P.; Guldi, D. M. *ChemPhysChem* **2002**, *3*, 195.

(20) (a) Kishida, H.; Hirota, K.; Wakabayashi, T.; Lee, B. L.; Kokubo, H.; Yamamoto, T.; Okamoto, H. *Phys. Rev. B* **2004**, *70*, 045402. (b) Greve, D. R.; Schougaard, S. B.; Geisler, T.; Petersen, J. C.; Bjornholm, T. *Adv. Mater.* **1997**, *9*, 1113. (c) Heflin, J. R.; Marciu, D.; Figura, C.; Wang, S.; Burbank, P.; Stevenson, S.; Dom, H. C. *Appl. Phys. Lett.* **1998**, *72*, 2788. (d) Coe, B. J.; Harris, J. A.; Brunschwig, B. S.; Asselberghs, I.; Clays, K.; Garin, J.; Orduna, J. *J. Am. Chem. Soc.* **2005**, *127*, 13399. (e) Yang, G.; Guan, W.; Yan, L.; Su, Z.; Xu, L.; Wang, E. B. *J. Phys. Chem. B* **2006**, *110*, 23092.

(21) (a) Wang, G. W.; Komatsu, K.; Murata, Y.; Shiro, M. *Nature* **1997**, *387*, 583. (b) Smith, A. B.; Tokuyama, H.; Strongin, R. M.; Furst, G. T.; Romanow, W. J.; Chait, B. T.; Mirza, U. A.; Haller, I. *Science* **1995**, *268*, 9359. (c) Zhao, Y.; Chen, Z.; Yuan, H.; Gao, X.; Qu, L.; Chai, Z.; Xing, G.; Yoshimoto, S.; Tsutsumi, E.; Itaya, K. *J. Am. Chem. Soc.* **2004**, *126*, 11134. (d) Yin, J. J.; Li, Y. G.; Li, B.; Li, W. X.; Jin, L. M.; Zhou, J. M.; Chen, Q. Y. *Chem. Commun.* **2005**, 3041.

(22) (a) Jin, X. L.; Xie, X. J.; Tang, K. L. *Chem. Comm.* **2002**, 750. (b) Nagao, S.; Kurikawa, T.; Miyajima, K.; Nakajima, A.; Kaya, K. *J. Phys. Chem. A* **1998**, *102*, 4495. (c) Nakajima, A.; Nagao, S.; Takeda, H.; Kurikawa, T.; Kaya, K. *J. Chem. Phys.* **1997**, *107*, 6491.

(23) Ma, B.; Riggs, J. E.; Sun, Y. P. *J. Phys. Chem. B* **1998**, *102*, 5999.

(24) (a) Patchkovskii, S.; Thiel, W. *J. Am. Chem. Soc.* **1998**, *120*, 556. (b) Andriotis, A. N.; Menon, M. *Phys. Rev. B* **1999**, *60*, 4521. (c) Andriotis, A. N.; Menon, M.; Froudakis, G. E. *Phys. Rev. B* **2000**, *62*, 9867. (d) Froudakis, G. E.; Andriotis, A. N.; Menon, M. *Chem. Phys. Lett.* **2001**, *350*, 393.

(25) Sawamura, M.; Iikura, H.; Nakamura, E. *J. Am. Chem. Soc.* **1996**, *118*, 12850.

(26) Nakamura, E. *J. Organomet. Chem.* **2004**, *689*, 4630.

(27) (a) Martin, H. D.; Mayer, B. *Angew. Chem., Int. Ed. Engl.* **1983**, *22*, 283. (b) Iikura, H.; Mori, S.; Sawamura, M.; Nakamura, E. *J. Org. Chem.* **1997**, *62*, 7912. (c) Matsuo, Y.; Tahara, K.; Nakamura, E. *Org. Lett.* **2003**, *5*, 3181.

(28) Chistyakov, A. L.; Stankevich, I. V. *J. Organomet. Chem.* **2000**, *599*, 18.

(29) (a) Pérez-Moreno, J.; Zhao, Y. X.; Clays, K.; Kuzyk, M. G. *Opt. Lett.* **2007**, *32*, 59. (b) May, J. C.; Biaggio, I.; Bures, F.; Diederich, F. *App. Phys. Lett.* **2007**, *90*, 251106. (c) Kolev, T.; Kityk, I. V.; Ebothe, J.; Sahraoui, B. *Chem. Phys. Lett.* **2007**, *443*, 309.

(30) (a) Velde, G. T.; Bickelhaupt, F. M.; Baerends, E. J.; Guerra, C. F.; Van Gisbergen, S. J. A.; Snijders, J. G.; Ziegler, T. *J. Comput. Chem.* **2001**, *22*, 931. (b) Guerra, C. F.; Snijders, J. G.; te Velde, G.; Baerends, E. J. *Theor. Chem. Acc.* **1998**, *99*, 391. (c) ADF 2006 01, SCM, Theoretical Chemistry, Vrije Universiteit, Amsterdam, The Netherlands. <http://www.scm.com>.

(31) Becke, A. D. *Phys. Rev. A* **1988**, *38*, 3098.

(32) Perdew, J. P. *Phys. Rev. B* **1986**, *33*, 8822.

(33) Vanleeuwen, R.; Baerends, E. J. *Phys. Rev. A* **1994**, *49*, 2421.

(34) (a) Vanlenthe, E.; Baerends, E. J.; Snijders, J. G. *J. Chem. Phys.* **1994**, *101*, 9783. (b) van Lenthe, E.; Ehlers, A.; Baerends, E. J. *J. Chem. Phys.* **1999**, *110*, 8943.

(35) (a) Orr, B. J.; Word, J. F. *Mol. Phys.* **1971**, *3*, 513. (b) Bishop, D. M. *J. Chem. Phys.* **1994**, *100*, 6535.

(36) Xu, Z. F.; Xie, Y. M.; Feng, W. L.; Schaefer, H. F. *J. Phys. Chem. A* **2003**, *107*, 2716.

(37) Haaland, A.; Nilsson, J. E. *Acta Chem. Scand.* **1968**, *22*, 2653.

(38) Coriani, S.; Haaland, A.; Helgaker, T.; Jorgensen, P. *ChemPhysChem* **2006**, *7*, 245.

(39) Herber, R. H.; Nowik, I.; Matsuo, Y.; Toganoh, M.; Kuninobu, Y.; Nakamura, E. *Inorg. Chem.* **2005**, *44*, 5629.

(40) Haaland, A.; Luszyk, J.; Novak, D. P.; Brunvoll, J.; Starowieyski, K. B. *J. Chem. Soc., Chem. Commun.* **1974**, 54.

(41) Brock, C. P.; Fu, Y. G. *Acta Crystallogr., Sect. B: Struct. Sci.* **1997**, *53*, 928.

(42) Kang, H. S. *J. Comput. Chem.* **2007**, *28*, 594.

(43) (a) Lein, M.; Frunzke, J.; Timoshkin, A.; Frenking, G. *Chem. Eur. J.* **2001**, *7*, 4155. (b) Kan, Y. H. *J. Mol. Struct.-Theochem.* **2007**, *805*, 127.

(44) Single points calculation at BP86/TZP optimized geometries using NBO 3.1 equipped in Gaussian 03, employing B3LYP/Lanl2dzECP for Fe atom and B3LYP/6-31G(d) for others.

(45) Waite, J.; Papadopoulos, M. G. *Z. Naturforsch., A: Phys. Sci.* **1987**, *42*, 749.

(46) (a) Kuzyk, M. G. *Phys. Rev. Lett.* **2000**, *85*, 1218. (b) Kuzyk, M. G. *Opt. Lett.* **2000**, *25*, 1183.

JP801305E